

Assessing the Dynamic Biofilm Removal of Sulfonated Phenolics using CP-OCT

K. Englund^a, J. Nikrad^b, R. Jones^{*a},

a University of Minnesota, School of Dentistry, Minneapolis, MN, 55455 USA

b Department of Microbiology and Immunology, University of Minnesota, Minneapolis, MN, 55455 USA

ABSTRACT

Examining the physical mechanisms related to biofilm removal of sulfonated phenolics (SP) is difficult using conventional microscopy techniques. A custom flow cell system integrated with a real time cross polarization optical coherence tomography system investigated the dynamic speed of biofilm removal when oral multi-species biofilms are exposed to SP under shear stress. The Near infrared 1310-nm CP-OCT system non-destructively imaged fluid immersed oral biofilms at nearly 30 frames/s. This dynamic imaging was able to determine the cohesive and adhesion related disruption of SP on oral biofilms adhering to tooth like surfaces. For multi-species biofilms that are initially grown without the presence of sucrose, the disruption of biofilms on saliva coated hydroxyapatite (HA) is dominated as an adhesive failure at the HA-biofilm interface. For multi-species biofilms that are grown in the presence of sucrose, the disruption is dominated by cohesive disruption followed by adhesive failure. This novel CP-OCT flow cell assay has the potential to examine rapid interactions between anti-biofilm agents and tooth like surfaces.

Keywords: Optical Coherence Tomography, Biofilm, Dentistry, Biofilm Disruption, Sulfonated Phenolics

1. INTRODUCTION

Many oral hygiene agents are effective plaque/biofilm growth inhibitors and/or reduce the attachment of salivary (planktonic) bacteria to the tooth surface¹⁻³. While there is clear benefit to the bacteriostatic effect of these agents⁴, the clinical efficacy of many of these agents is limited due to their poor ability to detach or disrupt established biofilms⁵. The contemporary view on oral biofilm management has deviated away from focusing on antimicrobials that kill bacteria or target specific organisms⁶. There are theoretical advantages in reducing specific caries associated bacteria (e.g. *Streptococcus mutans*) or periodontal associated bacteria (e.g. *Aggregatibacter actinomycetemcomitans*)^{7,8}, but since hard and soft tissue pathogenesis involves a complex ecology of bacteria, there is also a risk that anti-microbials can have unintended consequences. Both endodontics and periodontal treatment can involve needing additional antimicrobial/antibiotic agents to combat an acute or chronic infection. The possible unintended consequence of using these agents may involve detrimentally diminishing important commensal bacteria in the oral cavity. With the use of any systemic antimicrobial antibiotic agent for pre- or post- treatment of an endodontic or periodontal infection, there are additional concerns of affecting commensal and important bacteria in other parts of the body (e.g. gut flora)⁹.

For these reasons, microbiology research has focused heavily on agents that disrupt biofilms^{5,10}. While the concept seems rather straightforward, the process of creating and identifying effective agents that break up established biofilms is challenging. One reason for the difficulty is that most biofilms in nature exist as multi-species organisms, and these biofilms involve a diverse array of extracellular components^{11,12}. In other words, there isn't a *single molecular* target but an array of molecular bonds that are responsible for the cohesion and adhesion of the biofilm to the surface. While there are non-specific molecular approaches to reducing biofilm growth^{13,14}, there continues to be limited options for highly effective biofilm removal agents.

This paper will examine a professional application agent, a formulated sulfonated phenolics (SP), that can potentially be used to remove highly adherent biofilm. With the proper formulation, SP can be synthesized to be liquid desiccants and may be used for professional application treatment in periodontal therapy, endodontic therapy of permanent teeth, and chronic wounds.

* Corresponding Author: rsjones@umn.edu; phone +1 612-625-0395; Room 6-150 MoosT,1291A,515 Delaware St SE,Minneapolis, MN 5545

Our group has previously fabricated a flow cell system that is integrated with optical coherence tomography imaging for studying the detachment of oral biofilms in real time¹⁵. Optical Coherence Tomography (OCT) has been extensively investigated in the study of biofilms¹⁶⁻¹⁹. Our current project investigates how near infrared cross-polarization OCT (CP-OCT) can be utilized to image biofilm detachment in real-time through viscous and high refractive index solutions. The overall hypothesis of this work is that a specific SP, HYBENX® Decontaminant Solution (HBX), can rapidly remove multi-species biofilms from hydroxyapatite and that this rapid biofilm disruption performed in an *in vitro* flow cell can be imaged and quantified in real-time by CP-OCT.

2. METHODS

2.1 Multi-species Biofilms and Flow Cell System

This project uses a multi-species oral biofilm model to assess chemical disruption of the cohesive and adhesive characteristics of oral biofilms. While it is difficult to preserve the entire bacterial ecology of dental plaque, a significant portion of the plaque ecology can be preserved. These complex oral biofilms have the capability of preserving many of the phenotype features of *in vivo* biofilms. The Multi-Species Plaque Derived (MSPD) *in vitro* biofilm model used in this project is made from a dental plaque inoculum taken from a high caries risk child. In affiliate and IRB approved studies, we have characterized and banked a collection of MSPD *in vitro* biofilms²⁰⁻²².

These MSPD biofilms are grown from a frozen stock inoculum on saliva coated 5-mm hydroxyapatite discs and matured in a modified drip-flow reactor (DFR) system (BioSurface Technologies, Bozeman, MT)²³. Full description of the microbiology methods and images of the DFR system are described elsewhere²⁴. The DFR system re-creates the moist non-immersed plaque environment found in the oral cavity. The DFR is housed in a 37°C incubator. After 24 hours of biofilm growth, MSPD biofilms mature and grow to be several hundred microns thick and fully cover the discs. Since the HA discs can be removed from the custom slide jig, the biofilm coated HA discs can be transferred to a custom built flow cell. In a previous study, we first presented a custom flow cell that was fabricated to fit 5 mm diameter hydroxyapatite (HA) discs (Clarkson Chromatography, South Williamsport, PA). This flow cell was fabricated by milling polyetherimide (PEI). PEI has the chemical stability to be repeatedly autoclaved.

2.2 Characteristics of the Sulfonated Phenolics

Immediately after the biofilm coated HA discs are placed into the flow cell, the system is sealed to allow CP-OCT imaging. The flow cell has an input and output valve. The output valve is connected to plastic tubing that drains into a waste container. The input valve is connected to tubing that has a three way stop cock break in the line to allow for control of input fluid. Initially, 1X PBS is introduced into the flow cell which is then followed by a sulfonated phenolic (SP). Using a slight backflush technique, the SP can enter the tubing with minimal bubbles between the 1X PBS and the SP.

For this project we used a SP- HYBENX® Decontaminant Solution (HBX)-that is manufactured by Epien Medical (Saint Paul, MN). According to the MSDS from the manufacturer, HBX is a specific blend of hydroxybenzenesulfonics, sulfuric acid, and water. It is a highly viscous (1460 CPs) solution that is used with a syringe delivery system. The input flow rate was approximately 1 ml/sec for both 1X PBS and HBX.

2.3 Integrated Cross Polarization Optical Coherence Tomography Imaging

During the 1X PBS and SP flow, the flow cell was monitored with cross polarization optical coherence tomography (CP-OCT). This was feasible due to a glass window above the HA disc within the flow cell system. The CP-OCT system (IVS-200-CPM, Santec Co., Komaki, Japan) operates with a 30 kHz swept rate continuous wavelength scanning laser. The bandwidth of the 1310 nm center wavelength system is approximately 104 nm. The lateral resolution of the system based on the focusing optics within the probe housing was 80 microns²⁵. Schematics of the system have been previously reported^{25,26}, and interferometric concepts of swept source OCT imaging are well described elsewhere²⁷. Real-time imaging is realized by both the fast a-scan speed from the higher (relative standards) sweep rate and the acquisition speed in the x and y-axes of the Micro-Electro-Mechanical System (MEMS) scanning mirror in the body of the probe. The MEMS mirror is capable of collecting B-scans at 29 frames/second in both parallel and orthogonal orientation to the

flow direction within the flow cell. Biofilms were imaged in real-time parallel to flow during 1X PBS and SP (HBX) flow. ImageJ was used to analyze the real-time CP-OCT images²⁸.

2.4 Modeling Flow Forces Using Finite Element Modeling

In order to examine flow characteristics between PBS and HBX, the custom flow cell was finite element modeled using ANSYS Workbench 2.0 Framework, version 15.0.0 (2013, SAS IP, Inc.). We have previously described the finite element analysis method and the reasons for overall design of the flow cell¹⁵. The same ANSYS modelling was performed with the following settings in ANSYS Fluid Flow (Fluent) 15.0. First, the flow cell geometry dimensions were inputted and ANSYS automatically created the appropriate mesh for CFD (Fluent solver preference). The following input was required for Fluent: 1) The boundary conditions were a fluid velocity at the wall 0m/s in all directions, 2) Used pressure-based, absolute velocity formulation, 3) Viscous - Laminar setting, 4) Set fluid to have density of 996 kg/m³ and 1500 kg/m³ for 1x PBS and SP respectively, 5) Set viscosity of 0.001 kg/m-s and 0.96 kg/m-s for 1x PBS and SP respectively, 5) Set flow cell material to be PEI with a density of 1,270 kg/m³, 5) Set the following boundary conditions: wall, interior, outflow, and velocity – inlet was set at 60 ml/min (0.22668 m/s).

3. RESULTS

Our research design combines finite element analysis to characterize the flow characteristics of the initial wash of 1X PBS and the subsequent flow of our sulfonated phenolic (SP)-HYBENX® Decontaminant Solution (HBX). The ANSYS modelling results (Figure 1) characterized this dual liquid flow cell assay system where biofilms are first exposed to 1XPBS and the SP. Importantly, the design of our flow cell design was purposely done with an upward input and a downward output to create a laminar dominated flow characteristic. The right angle input direction is shown to dampen the turbulent flow that is created with the input (tube shaped) and main chamber (rectangular cross section). The parallel and orthogonal axes to the flow direction are visualized in the ANSYS modeling illustrations. The mean fluid velocities distribution at the center of the HA disc are shown in upper right of Fig 1. One factor is that the HYB viscosity significantly increases its shear force near the boundary of the HA disc, this in turn influences the velocity of HYB in the center of the flow cell. With the rate of the input and output valves being constant, this leads to a central velocity that is higher with HYB than 1XPBS (which is a water solution). This demonstrates how viscosity is closely connected to wall shear. This wall shear creates a slower fluid velocity at the peripheral which in turn creates a central higher velocity region. This modeling demonstrates the importance of assessing the biofilm heights across treatment groups since thicker biofilms will be subjected to higher velocities and shear stress. CP-OCT is able to rapidly assess and screen biofilm thickness.

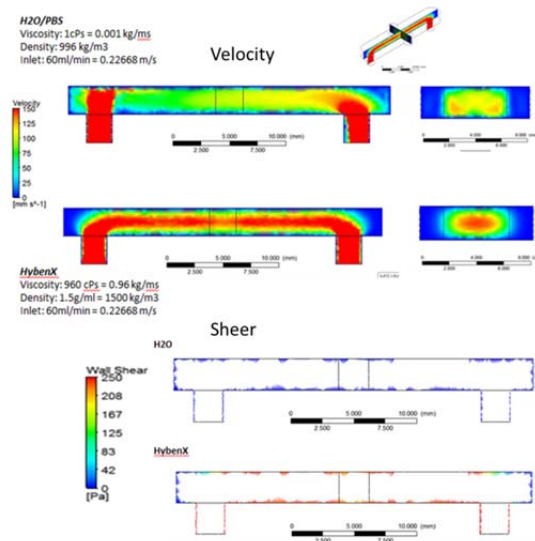


Figure 1. ANSYS finite element modeling of the velocity (top) and shear distribution (bottom) within the flow cell with 1XPBS/H2O versus sulfonated phenolic-HYBENX. The biofilm disc sits at the bottom of the flow cell in the central area (box area in center). HYB creates markedly high shear forces for biofilm removal.

The assay involves biofilms that are grown for 24 hours in a drip flow reactor and are transferred to the custom flow cell. In this flow cell, the assay is a two-step process: biofilms are first exposed to a 1X PBS and then exposed to a test liquid such as HYBENX. As in our previous study¹⁵, 1XPBS flow does not disrupt MSPD biofilms, regardless to addition/absence of sucrose during biofilm maturation. When HYBENX enters the flow cell, CP-OCT is able to image the nearly instantaneous removal of biofilms without previously sucrose exposure (not shown). This removal is from a ‘failure of adherence’ of the biofilm to the HA disc. CP-OCT can image this real-time adherence failure showing an almost immediately removal/ failure. However, the cohesive forces within the biofilm maintain the biofilm integrity. Biofilms that have been matured with 5% sucrose have higher extracellular matrix components. The 1310-nm based CP-OCT system can penetrate the full depth of these biofilms (in some cases over 1 mm in thickness). CP-OCT demonstrated that the sucrose exposed biofilms had a slight delay in their failure (Fig. 2A) with a brief time where the biofilms were being internally dispersed followed by adherence failure (Fig 2B).

Figure 3 illustrates how two biofilms-with and without previous sucrose exposure-are both effectively removed from the HA disc with HYBENX after a few seconds. But the removal from HYBENX is distinctly different when real-time CP-OCT analyzes the frame-by-frame images of the biofilms. The non-sucrose exposed biofilms almost immediately are disrupted through an adherence failure. The biofilm’s cohesive forces remain intact and the biofilm is visualized as being delaminated. The physical forces from the viscosity of the HBX likely cause this delamination. The viscosity of saline-based irrigation solutions at room temperature is approximately 1 centipoise (cPs) and the viscosity of HBX® at room temperature is 1460 cPs which is comparable to the viscosity of honey or glycerin. The high viscosity of HBX creates a high wall shear force that actively removes the non-sucrose exposed MSPD biofilm.

The sucrose exposed biofilm has a delay in ~ 5 seconds. While this may seem nominal and insignificant, examining the CP-OCT images that are captured at 29 frames/sec but analyzed at 7.5 frames/sec reveal that the sucrose biofilms are removed through a different process. CP-OCT images show a decrease in their scattering properties when exposed to HYB. The images look like the biofilms are dispersing internally before eventually the remaining portion is delaminated (Fig 2B). When we group the four studied MSPD biofilm samples (2 with sucrose exposure and 2 without sucrose exposure) and examine the biofilms after a few seconds of 1X PBS exposure, these biofilms are not removed. The biofilms encompass about $34.35\% \pm 7.26$ of the horizontal and vertical dimension of the flow cell system. We choose to examine only the tomographic plane parallel to the direction of flow. After examining up to 43.67 seconds of HYB flow into the flow cell, the MSPD biofilm coverage on the HA discs drops to $2.48\% \pm 1.45$. We did not run a completely separate group with 1XPBS only. Previous work has demonstrated the 1XPBS does not remove biofilm. Alongside, during the first stage of this assay, the 1XPBS does not remove biofilm. This demonstrates that the introduction of HYBENX is likely the sole cause of the rapid biofilm removal from the HA disc. We choose to precondition our assay with a few seconds of 1XPBS because the results of HYBENX alone were so rapid it was difficult to image the biofilm removal. The assay does require a syringe in the line that allows removing air bubbles prior to the 1XPBS and HYBENX entering the flow cell. The presence of air bubbles makes final analysis difficult with CP-OCT imaging. It is also important to consider that hydroxybenzenesulfonic alone has a high refractive index (~1.489), and the aqueous blend of HYBENX has an index of refraction ~1.42-1.45. This allows being able to identify the transition between 1X

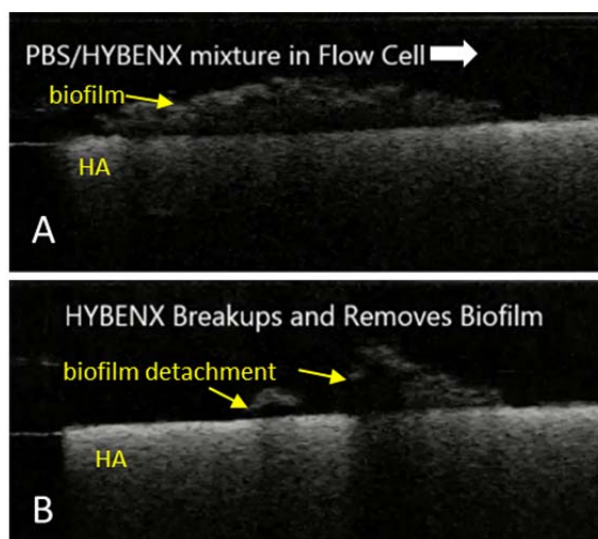


Figure 2. A) An adherent MSPD biofilm previously exposed to 5% sucrose exhibits initial resistance to removal with exposure to HYBENX within the custom flow cell. White arrow is flow direction. HA-hydroxyapatite B) After 5-6 seconds, the biofilm is internally dispersed and then detach from the HA.

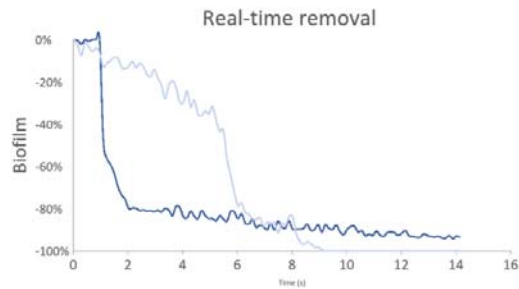


Figure 3. Real-time assessment of the biofilm removal allows examining how rapidly the non-sucrose biofilms (dark blue) will detach from the HA disks. Biofilms previously exposed to 5% sucrose for 24 hours (light blue) detach at a slower rate but the overall effect is pronounced.

PBS and HYBENX within the flow cell system.

4. CONCLUSION

The novelty of this work is related to how CP-OCT can image real-time interaction between solutions and biofilms that are hydrated in water. These biofilms can be imaged by CP-OCT through several millimeters of aqueous solution on top of the biofilm. This assay is innovative and allows assessing biofilms under laminar flow characteristics. Most biofilm removal, whether by an oral rinse, a periodontal or endodontal irrigant, is not under laminar flow conditions. Our Sulfonated Phenolics, HYBENX, that was used in this study is applicable to the oral environment as an endodontic irrigant, periodontal irrigant, and chronic wound irrigant. In all of these cases, the real-world application will produce turbulent flow within the rinse environment. But turbulent flow is difficult to reproduce across samples. Our *in vitro* laminar flow cell system produces flow conditions that test the inherent properties of the rinse or fluid. The goal is reproducibility. In this study's case, the sulfonate phenolic of HYBENX clearly has an almost immediate effect on biofilm removal through both its physical properties and a chemical desiccation effect. Both of these effects can be imaged and measured through testing biofilms with our custom integrated flow cell-CP-OCT assay. The chemical effect of the sulfonate phenolic is likely through a dehydrating mechanism. CP-OCT imaging is crucial in examining and measuring the effects of HYBENX in time and can assess the physical disruptive effects (cohesive versus adhesive). However, it is not a substitute for other levels of analysis that test the chemical mechanism. This can be assessed through formulation based testing (which CP-OCT can assist in examining) or other chemical assays. In summary, the integrated flow cell-CP-OCT imaging system assessed the rapid real-time effects of a sulfonated phenolic (HYBENX) on multi-species biofilms.

5. ACKNOWLEDGEMENTS

This work was supported through direct research funding to the University of Minnesota by EPIEN Medical Inc, Saint, Paul, MN. We would like to thank Michael Weston for his engineering prowess and the Minnesota Supercomputer Institute at the University of Minnesota for their computational resources.

6. REFERENCES

- [1] Finney, M., Walker, J.T., Marsh, P.D., and Brading, M.G., "Antimicrobial effects of a novel Triclosan/zinc citrate dentifrice against mixed culture oral biofilms.," *International dental journal* 53(6 Suppl 1), 371–8 (2003).
- [2] Rundegren, J., and Arnebrant, T., "Effect of delmopinol on the viscosity of extracellular glucans produced by *Streptococcus mutans*." *Caries research* 26(4), 281–5 (1992).
- [3] Tomás, I., Rubido, S., and Donos, N., [In situ antimicrobial activity of chlorhexidine in the oral cavity] , in *Sci. Against Microbial Pathog. Communicating Curr. Res. Technological Adv.*, A. Mendez-Vilas, Ed., Formatex, 530–541 (2011).
- [4] Hope, C.K., and Wilson, M., "Analysis of the Effects of Chlorhexidine on Oral Biofilm Vitality and Structure Based on Viability Profiling and an Indicator of Membrane Integrity" 48(5), 1461–1468 (2004).

- [5] Brindle, E.R., Miller, D.A., and Stewart, P.S., "Hydrodynamic deformation and removal of *Staphylococcus epidermidis* biofilms treated with urea, chlorhexidine, iron chloride, or DispersinB.," *Biotechnology and bioengineering* 108(12), 2968–77 (2011).
- [6] Davies, D., "Understanding biofilm resistance to antibacterial agents.," *Nature reviews. Drug discovery* 2(2), 114–22 (2003).
- [7] Koo, H., Xiao, J., Klein, M.I., and Jeon, J.G., "Exopolysaccharides produced by *Streptococcus mutans* glucosyltransferases modulate the establishment of microcolonies within multispecies biofilms.," *Journal of bacteriology* 192(12), 3024–32 (2010).
- [8] Suci, P., Kang, S., Gmür, R., Douglas, T., and Young, M., "Targeted delivery of a photosensitizer to *Aggregatibacter actinomycetemcomitans* biofilm.," *Antimicrobial agents and chemotherapy* 54(6), 2489–96 (2010).
- [9] Modi, S.R., Collins, J.J., and Relman, D.A., "Antibiotics and the gut microbiota.," *The Journal of clinical investigation* 124(10), 4212–8 (2014).
- [10] Chen, X., and Stewart, P.S., "Biofilm removal caused by chemical treatments," *Water Research* 34, 4229–4233 (2000).
- [11] Gross, E.L., Beall, C.J., Kutsch, S.R., Firestone, N.D., Leys, E.J., and Griffen, A.L., "Beyond *Streptococcus mutans*: dental caries onset linked to multiple species by 16S rRNA community analysis.," *PloS one* 7(10), e47722 (2012).
- [12] Langfeldt, D., Neuling, S.C., Heuer, W., Staufenbiel, I., Künzel, S., Baines, J.F., Eberhard, J., and Schmitz, R. a, "Composition of microbial oral biofilms during maturation in young healthy adults.," *PloS one* 9(2), e87449 (2014).
- [13] Quah, S.Y., Wu, S., Lui, J.N., Sum, C.P., and Tan, K.S., "N-acetylcysteine inhibits growth and eradicates biofilm of *Enterococcus faecalis*.," *Journal of endodontics* 38(1), 81–5 (2012).
- [14] Rasmussen, K., Nikrad, J., Reilly, C., Li, Y., and Jones, R.S., "N-Acetyl-l-cysteine effects on multi-species oral biofilm formation and bacterial ecology," *Letters in Applied Microbiology* 62(1), 30–38 (2016).
- [15] Rasmussen, K., Reilly, C., Li, Y., and Jones, R.S., "Real-time imaging of anti-biofilm effects using CP-OCT.," *Biotechnology and bioengineering* (2015).
- [16] Tóth, L., Vajas, A., Csomor, P., Berta, A., Sziklai, I., and Karosi, T., "Optical coherence tomography for biofilm detection in chronic rhinosinusitis with nasal polyposis," *European Archives of Oto-Rhino-Laryngology* 270(2), 555–563 (2013).
- [17] Blauert, F., Horn, H., and Wagner, M., "Time-resolved biofilm deformation measurements using optical coherence tomography," *Biotechnology and Bioengineering* 112(9), 1893–1905 (2015).
- [18] Haisch, C., and Niessner, R., "Visualisation of transient processes in biofilms by optical coherence tomography," *Water Research* 41(11), 2467–2472 (2007).
- [19] Xi, C., Marks, D., Schlachter, S., Luo, W., and Boppart, S.A., "High-resolution three-dimensional imaging of biofilm development using optical coherence tomography."

- [20] Rudney, J.D., Chen, R., Lenton, P., Li, J., Li, Y., Jones, R.S., Reilly, C., Fok, A.S., and Aparicio, C., "A reproducible oral microcosm biofilm model for testing dental materials.," *Journal of applied microbiology* 113(6), 1540–53 (2012).
- [21] Chen, R., Rudney, J., Aparicio, C., Fok, A., and Jones, R.S., "Quantifying dental biofilm growth using cross-polarization optical coherence tomography," *Lett Appl Microbiol* 54(6), 537–542 (2012).
- [22] Reilly C, Rasmussen, K., Selberg, T., Stevens, J., and Jones, R., "B," *Journal of Applied Microbiology*(in press), (2014).
- [23] Goeres, D.M., Hamilton, M.A., Beck, N.A., Buckingham-Meyer, K., Hilyard, J.D., Loetterle, L.R., Lorenz, L.A., Walker, D.K., and Stewart, P.S., "A method for growing a biofilm under low shear at the air-liquid interface using the drip flow biofilm reactor.," *Nature protocols* 4, 783–788 (2009).
- [24] Reilly, C., Rasmussen, K., Selberg, T., Stevens, J., and Jones, R.S., "Biofilm community diversity after exposure to 0.4% stannous fluoride gels," *Journal of Applied Microbiology* 117(6), 1798–1809 (2014).
- [25] Lenton, P., Rudney, J., Chen, R., Fok, A., Aparicio, C., and Jones, R.S., "Imaging in vivo secondary caries and ex vivo dental biofilms using cross-polarization optical coherence tomography," *Dent Mater* 28(7), 792–800 (2012).
- [26] Lenton, P., Rudney, J., Fok, A., and Jones, R.S., "Clinical cross-polarization optical coherence tomography assessment of subsurface enamel below dental resin composite restorations," *Journal of Medical Imaging* 1(1), 16001 (2014).
- [27] Liu, B., and Brezinski, M.E., "Theoretical and practical considerations on detection performance of time domain, Fourier domain, and swept source optical coherence tomography," *Journal of Biomedical Optics* 12(4), 44007–44012 (2007).
- [28] Abramoff, M.D., Magalhães, P.J., and Ram, S.J., "Image processing with imageJ," *Biophotonics International* 11, 36–41 (2004).